



Measurement report: Atmospheric Ice Nuclei at Changbai Mountain (2623 m a.s.l.) in Northeastern Asia

Yue Sun¹, Yujiao Zhu¹, Yanbin Qi², Lanxiadi Chen³, Jiangshan Mu¹, Ye Shan¹, Yu Yang¹, Yanqiu Nie¹, Ping Liu¹, Can Cui¹, Ji Zhang¹, Mingxuan Liu¹, Lingli Zhang⁴, Yufei Wang², Xinfeng Wang¹,
5 Mingjin Tang³, Wenxing Wang¹, Likun Xue¹

¹Environment Research Institute, Shandong University, Qingdao 266237, China

²Jilin Provincial Technology Center for Meteorological Disaster Prevention, Changchun 130062, China

³State Key Laboratory of Organic Geochemistry, Guangzhou Institute of Geochemistry, Chinese Academy of Sciences, Guangzhou 510640, China

10 ⁴Changbai Mountain Meteorological Observatory, An Tu, Jilin 133613, China

Correspondence to: Yujiao Zhu (zhuyujiao@sdu.edu.cn), Likun Xue (xuelikun@sdu.edu.cn)

Abstract. Atmospheric ice nucleation plays an important role in modifying the global hydrological cycle and atmospheric radiation balance. To date, few comprehensive field observations of ice nuclei have been carried out at high-altitude sites, which is close to the height of mixed-phase cloud formation. In this study, we measured the concentrations of ice-nucleating
15 particles (INPs) in the immersion freezing mode at the summit of Changbai Mountain (2623 m above sea level), Northeast Asia, in summer 2021. The cumulative number concentration of INPs varied from $3.8 \times 10^{-3} \text{ L}^{-1}$ to 2.3 L^{-1} over the temperature range from $-20.5 \text{ }^\circ\text{C}$ to $-5.5 \text{ }^\circ\text{C}$. Proteinaceous-based biological materials accounted for the majority of INPs, with the proportion of biological INPs (bio-INPs) exceeding 75% across the entire freezing temperature range, with this proportion even exceeding 90% above $-13.0 \text{ }^\circ\text{C}$. At freezing temperatures ranging from $-11 \text{ }^\circ\text{C}$ to $-8 \text{ }^\circ\text{C}$, bio-INPs were
20 found to significantly correlate with wind speed and Ca^{2+} , and weakly correlate with isoprene and its oxidation products (isoprene $\times \text{O}_3$), suggesting that biological aerosols may attach to soil dust surfaces and contribute to INPs. During the daytime, bio-INPs showed a positive correlation with the planetary boundary layer height, with the valley breezes from southwestern mountainous regions also influencing the concentration of INPs. Moreover, the long-distance transport of air mass from the Japan Sea and South Korea significantly contributed to the high concentrations of bio-INPs. Our study
25 emphasizes the important role of biological sources of INPs in the high-altitude atmosphere of northeastern Asia, as well as the significant contribution of long-range transport to the INPs concentrations in this region.

1 Introduction

Clouds play a crucial role in regulating the Earth's energy balance by absorbing, reflecting, and scattering solar and terrestrial radiation (Zhou et al., 2016; Bjordal et al., 2020). As most precipitation in clouds initiates via the ice phase, it is
30 important to study the formation of ice in clouds (Kanji et al., 2017). Atmospheric aerosols can act as ice-nucleating particles (INPs), triggering the freezing of cloud droplets through heterogeneous nucleation processes (Rinaldi et al., 2017; Koop et



al., 2000; Rosenfeld and Woodley, 2000; Demott et al., 2003; Cziczo et al., 2013; Murray et al., 2010). Currently, the four main mechanisms of heterogeneous ice nucleation are considered: deposition nucleation, condensation freezing, immersion freezing, and contact freezing (Demott et al., 2003; Vali et al., 2015). Recent studies have concluded that water saturation is a prerequisite for ice formation in mixed-phase clouds, and that contact and immersion freezing are the most primary pathways for ice formation (Sassen and Khvorostyanov, 2008; Phillips et al., 2007; Murray et al., 2012).

Various aerosol particles are potential INPs, such as biological aerosols (Pratt et al., 2009; Tobo et al., 2013), mineral dusts (Pratt et al., 2009; Atkinson et al., 2013), sea spray aerosols (Mccluskey et al., 2017; Alpert et al., 2022), carbonaceous aerosols (Grawe et al., 2018; Demott, 1990; Diehl and Mitra, 1998; Fornea et al., 2009), volcanic ashes (Grawe et al., 2016; Umo et al., 2015), etc. It is generally demonstrated that biological aerosols, which have proteins embedded in their outer membranes, are the most efficient INPs at temperatures above -15°C (Petters and Wright, 2015; Murray et al., 2012; Huang et al., 2021). For example, lichens can induce freezing above -10°C (Moffett et al., 2015), and some bacterial organisms like *Pseudomonas syringae* can facilitate droplet freezing at extremely high temperatures (above -2°C) (Maki et al., 1974). At -15°C , biological aerosols can contribute to more than 70% of INPs according to studies in mountain sites (Gong et al., 2022), urban areas (Chen et al., 2021), and agricultural soils (Testa et al., 2021). Non-proteinaceous biological particles, such as pollen, cellulose, and other macromolecular organic particles, can also induce ice formation through heat-resistant polysaccharides on their surfaces, but at lower temperatures than proteinaceous biological particles (Knopf et al., 2010; Pummer et al., 2012). Mineral dust dominates the INPs concentrations at low freezing temperatures, with feldspar being one of the most effective mineral dusts for ice nucleation below -15°C (Atkinson et al., 2013; Augustin-Bauditz et al., 2016). However, feldspar minerals can also act as INPs at higher temperatures depending on several factors, including their chemical composition, crystal structures, atmospheric abundance, type of solute molecules, and particle concentration per droplet in the immersion freezing mode (Harrison et al., 2016; Whale et al., 2018), etc. The ice-nucleating properties of aerosols are affected by many factors. For instance, the size of particles is a crucial factor for providing active sites for ice formation, with larger particles containing more efficient ice nucleation sites than smaller ones (Chen et al., 2018; Demott et al., 2010; Demott et al., 2015). In addition, the chemical composition and surface properties of aerosol particles, such as their surface topology, defects, roughness, and functional groups, also influence their activity as INPs (Freedman, 2015; Kanji and Abbatt, 2010; Mahrt et al., 2018; Roudsari et al., 2022). Furthermore, the ice-nucleating properties of aerosol particles can be modified through chemical reactions with trace gases or organic/inorganic component or through physical processes such as efflorescence or deliquescence (Cziczo et al., 2009; Hoose and Möhler, 2012; Creamean et al., 2013; Tang et al., 2016; Tang et al., 2018).

Over recent decades, numerous studies have focused on investigating heterogeneous ice nucleation in various atmosphere environments. In low-altitude atmospheres, the abundance of ground-based sources and sinks results in spatial distribution heterogeneity, which restricts the characterization of INPs properties on a regional scale. At present, it is unclear whether INPs capable of ice formation at ground level can be transported to the altitudes of mixed-phase cloud formation



65 (approximately 3–7 km). High-altitude sites provide favorable conditions for in situ observations to investigate INPs
characteristics, as they can represent tropospheric background conditions and reflect long-distance transport and vertical
mixing processes prior to arriving at the ground sampling site. Therefore, field experiments have been conducted in several
high-altitude sites. For example, in the Swiss Alps, simultaneous measurements taken at different-altitude stations revealed a
70 reduction of approximately 50% per kilometer in the abundance of INPs in the vertical gradient (ranging from 489 m above
sea level (a.s.l.) to 3580 m a.s.l.) in the warm season (Conen et al., 2017). This decline in INPs could even reach one order of
magnitude during the cold season (from 1631 m a.s.l. to 2693 m a.s.l.) (Wieder et al., 2022), which was attributed to the
scarcity of effective INPs sources in high-altitude atmospheres. In contrast, Schrod et al. (2017) reported an increase in INPs
abundance of approximately 10 times over the eastern Mediterranean (2500 m a.s.l.) relative to ground level using unmanned
aircraft systems, with this difference attributed to the long-distance transport of dust particles at the height of a few
75 kilometers. In mountainous areas with high vegetation coverage, biogenic aerosols are the most abundant type of INPs. For
example, at the Jungfraujoch station (3580 m a.s.l.) in the Swiss Alps, approximately 80% of INPs were biological aerosols
at freezing temperatures above -15°C . Similarly, at the Puy de Dôme station (1465 m a.s.l.) in France, the average
contribution of biological aerosols in cloud water could reach up to 85% at freezing temperatures above -10°C (Joly et al.,
2014). To date, fewer field observations have been carried out in high-altitude regions in China. For example, Jiang et al.
80 (2014, 2015) performed measurements at Mt. Huangshan (1840 m a.s.l.) in Southeast China, finding that larger particles
were more likely to be effective INPs and establishing a parametric equation that depends on temperature and ice
supersaturation for predicting the INPs concentration. Lu et al. (2016) collected seven rainwater samples from three
mountains in eastern China, i.e., Changbai Mountain (2740 m a.s.l.), Wuling Mountain (900 m a.s.l.), and Dinghu Mountain
(1000 m a.s.l.), and found that the initiated freezing temperature was approximately -6°C , but bacteria played minor roles in
85 the overall INP activity. Because the number of rainwater samples was limited, further research is necessary to explore the
impact of biological INPs on cloud droplets and their contribution to the formation of precipitation.

In this study, we conducted offline INPs measurements at the top of Changbai Mountain (2623 m a.s.l.) in Jilin
province, China, which is located in Northeast Asia. This region is particularly vulnerable to climate change because of the
presence of distinct ecotones caused by land type changes, as well as the influence of the North Atlantic Oscillation and the
90 Northern Hemisphere circulation (Sugita et al., 2007; Zhang et al., 2021). Moreover, Northeast Asia is densely populated
and serves as a crucial breadbasket for the world, making rainfall an essential factor for determining crop yields. Given the
high altitude of Changbai Mountain, it is an ideal location to capture the characteristics of the regional atmospheric
background and transboundary transport of air mass. Our main objective was to investigate the concentration levels of INPs
and identify their major sources at the height of the mountain's peak. Additionally, we evaluated the impact of the planetary
95 boundary layer (PBL) height, valley breezes, and transport pathways of INPs to gain a better understanding of INPs sources
in this region. Our findings could provide valuable insights into the formation and behaviour of clouds over this region.



2 Methods

2.1 Site description

Changbai Mountain is the highest mountain in the border region between China and the Korean Peninsula. It is situated on the transport pathways of continental air pollutants from Asia to the North Pacific Ocean and even as far as the Arctic. The regional topography is characterized by forests and mountains, with elevations ranging from 410 m a.s.l. to 2740 m a.s.l., gradually decreasing from the southeast to the northwest. At the top of Changbai Mountain, there is a vast crater known as Tianchi Lake, which has a depth of 373 m and covers an area of 9.82 km². In this study, a field campaign was carried out at the Tianchi Meteorological Station (Tianchi Site, 42.03°N, 128.08°E, 2623 m a.s.l., Figure 1), which is approximately 150 m northeast of Tianchi Lake, from July 25 to August 21, 2021.

Changbai Mountain is in a typical temperate continental mountain climate influenced by the monsoon, with long cold winters and short temperate summers. The annual average temperature is typically lower than -7.4 °C (Jin et al., 2018), with the mountain summit always covered by snow and ice for approximately three quarters of the year. During the campaign, the relative humidity (RH) ranged from 33% to 100%, with a mean of $94.6 \pm 10.0\%$. Notably, eighty percent of the RH exceeded 90% throughout the campaign, indicating that the campaign was performed under humid weather conditions. The sampling site was predominantly affected by southerly and southwesterly winds, with wind speed (WS) ranging from 0.1 m s⁻¹ to 17.5 m s⁻¹. Changbai Mountain is a national nature reserve with no large industrial facilities nearby. The surroundings of the observation site are covered by dense vegetation, such as shrubs and perennial herbs, but with few anthropogenic activities. Most of the time, the site is above the PBL and in the free troposphere, making it an ideal site for studying the regional background atmosphere of Northeast Asia.

2.2 Sample collection

Bulk aerosol particles were collected on polycarbonate (PCTE) membrane filters (Sterlitech 1870, nominal porosity 0.45 μm) using a TH-150D medium flow sampler (Wuhan Tianhong Corporation, China) at a flow rate of 50 L min⁻¹. Samples were collected during the daytime (06:00 to 17:30) and nighttime (18:00 to 05:00 in the following day). A total of 24 samples were collected on PCTE filters. Meanwhile, fine particulate matter (PM_{2.5}) samples were collected on quartz microfiber filters (PALL Pallflex, 7204), which were heated at 560 °C for 4 h before sampling to remove any adsorbed organics, using another medium flow sampler (Wuhan Tianhong Corporation, China) with a 2.5 μm impactor at a flow rate of 100 L min⁻¹. A total of 157 samples were collected on quartz filters every 3 h. After sampling, all filter samples were kept frozen at ≤ -18 °C until analysis.

Real-time measurements of PM_{2.5} and black carbon (BC) were recorded at 1 min intervals by using SHARP 5012 (Thermo Scientific, USA) and SHARP 5030 (Thermo Scientific, USA), respectively. Trace gases including CO, SO₂, NO_x, and O₃, were detected using Thermo Scientific 48i, 43i, 42i, and 49i, respectively. Ambient volatile organic compounds



(VOCs) were collected by taking air samples using stainless-steel canisters with a time resolution of 12 h on clean days and 3 h on polluted days. Meteorological data, such as temperature, humidity, WS, wind direction, pressure, and precipitation, were monitored by the Tianchi weather station.

2.3 INPs analysis

INP measurements in the immersion mode were conducted using the Guangzhou Institute of Geochemistry Ice Nucleation Apparatus (GIGINA) from -40 °C to 0 °C. GIGINA is a cold-stage-based ice nucleation array that consists of a commercial cold stage, an enclosed droplet chamber (LTS120, Linkam, Epsom Downs, UK), an external refrigerated water circulator (VIVO RT4, Julabo, Seelbach, Germany), a charge-coupled device (CCD) camera (DMK33G274, The Imaging Source, Bremen, Germany), a ring LED light, and a computer system. Further details regarding GIGINA have been published by Chen et al. (2023).

Each polycarbonate filter was immersed in 5 mL MilliQ water (resistivity of 18.2 M Ω cm $^{-1}$ at 25 °C) and sonicated for 30 min to wash off particles (Chen et al., 2021). Note that an ice water bath was utilized during ultrasonic extraction to mitigate any potential alterations in protein properties and biogenic activities. The INPs measurement process is briefly described as follows. First, a hydrophobic glass slide was placed on a cold stage and filled with silicone oil to achieve good thermal contact. Second, a round aluminum spacer with 90 round compartments was placed on the glass slide, and the particle suspension was sequentially pipetted into each compartment. Then, another glass slide was placed above the spacer to avoid the Wegener–Bergeron–Findeisen process (Jung et al., 2012). Afterward, the temperature of the droplets was cooled down to 0 °C at a cooling rate of 10 °C min $^{-1}$, after which the cooling of the droplets continued at a rate of 1 °C min $^{-1}$ until all the droplets were frozen. During the freezing experiment, high-purity nitrogen was continuously delivered onto the cold stage to prevent frost from forming on the surface of the glass slide. Meanwhile, real-time images of the droplets were photographed by the CCD camera and recorded by the LINK software every 6 s. After the experiment, the phase transition of each droplet was identified by analyzing the changes in image brightness, which distinguished between unfrozen (white) and frozen (dark) droplets.

The frozen fraction, f_{ice} , was calculated according to Eq. (1):

$$f_{ice}(T) = \frac{n_{ice}}{n_{tot}}, \quad (1)$$

where n_{ice} is the number of frozen droplets above temperature T , and n_{tot} is the total number of droplets (90 droplets). The cumulative concentration of each droplet above K (T), and the cumulative number concentration of INPs (N_{INP}) in the unit volume of sampled air, were calculated following the method of Vali (1971, 2015):

$$K(T) = -\frac{\ln[1-f_{ice}(T)]}{V} (\text{cm}^{-3} \text{ of water}), \quad (2)$$

$$N_{INP}(T) = -\frac{\ln[1-f_{ice}(T)]}{V_{air}} (\text{L}^{-1} \text{ air}), \quad (3)$$



where V is the volume of each droplet (1 μL), and V_{air} is the total volume of sampled air per droplet converted to standard conditions (0 $^{\circ}\text{C}$ and 1013 hPa). In our study, the N_{INP} values were significantly larger in filter samples than in the field blanks.

The rarity of INPs in the atmosphere leads to their low concentration in the suspension. Because the suspension used in the measurement contained a limited number of droplets, we need to consider the resulting uncertainty for estimating N_{INP} in both the whole suspension and thus the atmosphere. Additionally, the uncertainty associated with the droplet-freezing apparatus cannot be ignored. To address these uncertainties, we calculated the confidence intervals of the apparatus for f_{ice} according to the method of Gong et al. (2022) and Agresti and Coull (1998):

$$\left(f_{\text{ice}} + \frac{Z_{\alpha/2}^2}{2n_{\text{tot}}} \pm Z_{\alpha/2}^2 \sqrt{[f_{\text{ice}}(1 - f_{\text{ice}}) + Z_{\alpha/2}^2/(4n_{\text{tot}})]/n_{\text{tot}}} \right) / (1 + Z_{\alpha/2}^2/n_{\text{tot}}), \quad (4)$$

where $Z_{\alpha/2}$ is the standard score at a confidence level $\alpha/2$, for which the 95% confidence interval is 1.96.

2.4 Chemical analysis

The $\text{PM}_{2.5}$ samples collected by quartz membranes were used to analyze the particle chemical composition. For each sample, an eighth of the filter was ultrasonically extracted using 15 mL MilliQ water for 30 min to make a suspension. The concentrations of inorganic water-soluble anions (Cl^- , SO_4^{2-} , and NO_3^-) and cations (Na^+ , NH_4^+ , K^+ , Mg^{2+} , and Ca^{2+}) were identified using the ICS 1100 ion chromatograph (Thermo Scientific). In addition, the concentrations of organic carbon (OC) and elemental carbon (EC) were measured using the Sunset Laboratory Model-5 semi-continuous OC/EC field analyzer. The VOCs canister samples were analyzed using online gas chromatography–mass spectrometry (TT24xr, Makers, UK; GC–MS, Thermo Scientific, USA) in the laboratory. A total of 106 target VOCs, including 29 alkanes, 11 alkenes, one alkyne, 17 aromatics, 35 halogenated hydrocarbons and 13 oxygenated VOCs (OVOCs), were quantified.

2.5 The PBL data and air mass back trajectory model

The PBL data were downloaded from the Climate Data Store (<https://cds.climate.copernicus.eu>), which provides hourly records on latitude–longitude grids at $0.25^{\circ} \times 0.25^{\circ}$ resolution. The 72 h air mass backward trajectories at the sampling sites were calculated using the Hybrid Single Particle Lagrangian Integrated Trajectory (HYSPLIT) model (<http://ready.arl.noaa.gov/HYSPLIT.php>), which is developed by the National Oceanic and Atmospheric Administration Air Resources Laboratory (NOAA ARL) (Stein et al., 2015). The simulations were based on meteorological data from the Global Data Assimilation System (GDAS) with a spatial resolution of $1^{\circ} \times 1^{\circ}$ and an end altitude of the backward trajectory of 2623 m a.s.l. Using the open-source software of MeteoInfo, concentration-weighted trajectory (CWT) analysis was conducted to explore the potential sources of INPs based on the air mass backward trajectories and N_{INP} . Note that uncertainty may exist in the CWT analysis due to the relatively small dataset of INPs in this study.



3 Results and Discussion

3.1 INP concentrations

190 A metric was applied to characterize the situation of droplet freezing, i.e., the freezing temperature at which 50% of the droplets are frozen (T_{50}). The frozen fractions (f_{ice}) of all freezing curves containing the collected samples and MilliQ water are shown in Figure 2a. The T_{50} of MilliQ water ranged from -30.0 °C to -28.5 °C, reflecting the low background value of the droplet-freezing apparatus. For the two blank filters, T_{50} was averaged to -23.0 ± 0.7 °C, which was slightly higher than that of MilliQ water, but much lower than that of the collected samples (for which T_{50} was -13.0 ± 1.5 °C), indicating that
195 the sparse contaminants from the filter membrane can be ignored. In the following analysis, the concentrations of the two blank filters were subtracted from the daytime and nighttime samples, respectively.

The N_{INP} values as a function of temperature are presented in Figure 2b, where the pink and blue circles represent the samples collected during the daytime and nighttime, respectively. The freezing of ambient samples was observed in the temperature range of -26.0 °C to -5.5 °C, with N_{INP} spanning three orders of magnitude from $3.8 \times 10^{-3} \text{ L}^{-1}$ to 2.3 L^{-1} . For
200 freezing temperatures above T_{50} , the temperature region is referred to as the high-temperature region (HTR), where N_{INP} spans three orders of magnitude from $3.8 \times 10^{-3} \text{ L}^{-1}$ to 0.8 L^{-1} , indicating the diversity of INP populations and sources in this temperature range. Some of the N_{INP} curves rose sharply in the HTR, which could be due to a strong local source of INPs. A similar phenomenon was also observed at a coastal site (the Cape Verde Atmospheric Observatory, Africa) by Welti et al. (2018) in air samples and in the upper bound of the composite nucleus spectrum of cloud water and precipitation samples by
205 Petters and Wright (2015). In contrast, in the low-temperature region (LTR, freezing temperatures below T_{50}), N_{INP} showed a relatively narrow variation from $3.6 \times 10^{-2} \text{ L}^{-1}$ to 2.3 L^{-1} . The temperature dependence of the spectra reflects the complexity of the INP sources. Furthermore, there were no significant differences observed in N_{INP} between daytime and nighttime. However, in some mountainous sites, such as Mt. Huang (Jiang et al., 2015) and the Alps (Wieder et al., 2022), N_{INP} displayed a distinct diurnal cycle induced by the orographically lifted air masses containing high INP concentrations from
210 low elevation upstream during the daytime. The absence of an INPs diurnal cycle at the top of Changbai Mountain may be due to its surrounding high-altitude terrain and the weak convection from the mountain base.

We compared our N_{INP} measurements with previous results from diverse sites. For instance, in mountainous regions, the N_{INP} value at the Alps varied from 10^{-4} to 10^0 , and the temperature spectra showed a wider range (Wieder et al., 2022). In our observations, the spectra of N_{INP} were narrowly located in the relatively high-temperature and high-concentration regions.
215 Jiang et al. (2015) reported the INPs concentrations at the top of Mt. Huang, where the temperature spectra of N_{INP} were much narrower than those at the Alps. While the N_{INP} spectra at Mt. Huang partially overlapped with our results in the temperature range from -15 °C to -20 °C, the N_{INP} value was much larger at Mt. Huang than our results. Gong et al. (2022)



measured INPs at the mountain station at Cerro Mirador (622 m a.s.l., Chile), and reported N_{INP} values lower than those in our study by around one order of magnitude, while the freezing temperatures measured (from -25.0 °C to -3.0 °C) were similar to our study. In heavily polluted urban sites, such as Beijing (Chen et al., 2018) and Tai'an (Jiang et al., 2020) in China, the INPs concentrations were comparable to our measurements at overlapping freezing temperatures. Chen et al., (2018) reported that INPs concentrations might not be influenced by urban air pollution because no correlation was found between the immersion-freezing nuclei concentration and the $\text{PM}_{2.5}$ or BC concentration. Carbonaceous particles might not act as efficient INPs in the immersion mode or may decrease ice nucleation activity because of the formation of organic coatings in polluted urban environments with complex aerosol sources (Schill et al., 2020; Nishman et al., 2019; Hammer et al., 2018).

3.2 Contribution of biological particles, other organics, and inorganics to INPs

Generally, biological particles can induce ice nucleation in the immersion mode at relatively high temperatures above -15.0 °C (Murray et al., 2012). Proteinaceous components mainly induce biological ice nucleation, and wet heat treatment (i.e., heating the particle suspension to 95.0 °C for 30 min) is used to identify the protein-based biological ice nucleation activity (Beall et al., 2022; Chen et al., 2021). We measured the N_{INP} values of the suspensions after heat treatment, which we refer to as heat-resistant N_{INP} ($N_{\text{INP-heat}}$), and the difference between the original N_{INP} and $N_{\text{INP-heat}}$ was considered to be mainly due to the proteinaceous biological N_{INP} ($N_{\text{INP-bio}}$). However, some biological aerosols, such as pollen, cellulose, or other macromolecular organic particles, are insensitive to heat treatment at 95.0 °C (Daily et al., 2022). Therefore, we also measured the heat-stable organic INPs, which are defined as other organic INPs (other org-INPs), following the methods of Suski et al. (2018) and Testa et al. (2021). We added 30% H_2O_2 (Sigma Aldrich) to the suspension to obtain a final concentration of 10%, and then heated it at 95 °C for 20 min under UVB fluorescent bulbs. To prevent freezing point depression, we neutralized the remaining H_2O_2 in the suspension with catalase. The N_{INP} value following treatment by this procedure was denoted H_2O_2 -resistant N_{INP} ($N_{\text{INP-H}_2\text{O}_2}$), which is the concentration of inorganic INPs ($N_{\text{INP-inorg}}$). The difference between heat-resistant N_{INP} and H_2O_2 -resistant N_{INP} was considered to be equivalent to the concentration of other organic INPs ($N_{\text{INP-other org}}$).

Figure 3 illustrates the concentrations and fractions of the three types of INPs. The biological INPs (bio-INPs) showed ice nucleation activity at temperatures between -20 °C and -5.5 °C. After the ice nucleation activity of the bio-INPs was destroyed, $N_{\text{INP-heat}}$ decreased by around 1–2 orders of magnitude compared with the original N_{INP} , indicating a significant contribution of $N_{\text{INP-bio}}$. The initial freezing temperature of other org-INPs was -13.5 °C, which was approximately 8 °C lower than that of bio-INPs. Inorganic INPs exhibited ice nucleation activity at temperatures between -25.5 °C and -10 °C, and were found to dominate the ice nucleation below -23.5 °C. Interestingly, the initial freezing temperatures of some inorganic INPs were slightly higher than those of other org-INPs, indicating that some inorganic aerosols could trigger freezing at relatively high temperatures.



250 The proportions of the three types of INPs as functions of temperature are presented in Figure 3(c). Here, the fractions
of $N_{\text{INP-bio}}$ ($F_{\text{INP-bio}}$) account for 100% of the N_{INP} value above $-11\text{ }^{\circ}\text{C}$, and show a decreasing trend as the temperature
decreases from $-11.5\text{ }^{\circ}\text{C}$ to $-16.5\text{ }^{\circ}\text{C}$. This decreasing trend of $F_{\text{INP-bio}}$ is consistent with trends observed in other areas
dominated by bio-INPs in similar temperature regions (Gong et al., 2022; O'sullivan et al., 2018; Testa et al., 2021),
suggesting that the ice nucleation activity of bio-INPs decreases with decreasing temperature. Interestingly, when the
255 temperature decreased from $-16.5\text{ }^{\circ}\text{C}$ to $-20.0\text{ }^{\circ}\text{C}$, the median of $F_{\text{INP-bio}}$ increased from 0.8 to 0.9, indicating the presence of
INPs with relatively high ice-nucleating activity in the LTR. Previous observational studies have indicated that although
most bio-INPs act as ice nuclei at high freezing temperature, some heat-sensitive biological aerosols, such as fungal cloths,
exhibit ice-nucleating activity at low temperatures (Iannone et al., 2011; Kanji et al., 2017). Modeling studies have also
shown that bio-INPs can influence the ice phase of clouds and produce ice crystals when the cloud-top temperature is below
260 $-15\text{ }^{\circ}\text{C}$ (Hummel et al., 2018). This phenomenon may also be related to the sensitivity of different species of biological
aerosol to heating conditions. In wet heat treatment it is assumed that the ice-nucleating active protein in bio-INPs is
completely destroyed and denatured, thus losing any ice formation potential. However, this method may lead to decrease in
the freezing temperature of bacteria and fungi, but their ice-forming activity still cannot be ignored (Daily et al., 2022). Note
that the number of samples was less than 50% at some temperatures, resulting in uncertainties in these temperature ranges
265 (light color shown in Figure 3c). Overall, the median value of $F_{\text{INP-bio}}$ was more than 75% in the entire temperature range
from $-20.5\text{ }^{\circ}\text{C}$ to $-5.5\text{ }^{\circ}\text{C}$, with the value exceeding 90% above $-13.0\text{ }^{\circ}\text{C}$, which was much higher than in some mountainous
areas in southwestern South America (Gong et al., 2022) and urban areas in China (Chen et al., 2021). The fractions of $N_{\text{INP-}}$
 other org ($F_{\text{INP-other org}}$) showed an opposite trend from that of $F_{\text{INP-bio}}$ at freezing temperatures between $-20.0\text{ }^{\circ}\text{C}$ and $-13.5\text{ }^{\circ}\text{C}$.
First, $F_{\text{INP-other org}}$ increased from 0.08 to 0.3 as the temperature decreased from $-13.5\text{ }^{\circ}\text{C}$ to $-18\text{ }^{\circ}\text{C}$, and then sharply
270 decreased from 0.3 to 0.08 as the temperature decreased further from $-18.5\text{ }^{\circ}\text{C}$ to $-20.0\text{ }^{\circ}\text{C}$. The fractions of $N_{\text{INP-inorg}}$ ($F_{\text{INP-}}$
 inorg) remained below 0.15 throughout the entire temperature range, which is consistent with previous studies in some clean
atmospheres. Overall, our results showed that protein-based biological aerosols contribute the most to INPs at Changbai
Mountain.

3.3 Source analysis of different types of INPs

275 We investigated the relationship between different types of INPs and various environmental conditions, as well as the
gases and particle compositions. Our results showed that there were significant positive correlations between N_{INP} and WS in
the temperature range from $-12\text{ }^{\circ}\text{C}$ to $-9\text{ }^{\circ}\text{C}$. High WS can enhance the uplift of soil dust and the long-distance transport of
aerosols. Moreover, N_{INP} and Ca^{2+} showed a good positive correlation in the HTR, suggesting that soil dust may play an
important role in ice nucleation in this temperature range. Previous studies have shown that when soil dusts mix with
280 biological components, their freezing temperatures can increase to as high as $-6\text{ }^{\circ}\text{C}$, which is much higher than that of
natural dust (below $-20\text{ }^{\circ}\text{C}$) (Kanji et al., 2017). In contrast, N_{INP} exhibited no correlations with $\text{PM}_{2.5}$, BC, or water-soluble



species like sulfate, nitrate, and ammonium (SNA), suggesting that BC and inorganic particulate components are not active INPs.

We also investigated the potential sources of different types of INPs, as shown in Figure 4(b–d). Similar to the total
285 INPs, $N_{\text{INP-bio}}$ showed a significant positive correlation with WS and Ca^{2+} at temperatures ranging from $-11\text{ }^{\circ}\text{C}$ to $-8\text{ }^{\circ}\text{C}$, as well as a weak positive correlation with isoprene and its oxidation products ($\text{isoprene} \times \text{O}_3$). O'sullivan et al. (2016) and Augustin-Bauditz et al. (2016) reported that biological materials may attach to or mix with dust particles and promote INPs formation. However, no mineral dust events were observed during our sampling period, based on the low mass concentrations of $\text{PM}_{2.5}$ and metal ions. We speculate that the source of bio-INPs was related to soil dust. The higher WS
290 may have facilitated the exposure of the local soil dust and bioaerosol containing bio-INPs to the air. Alternatively, the long-distance transport of biological aerosol attached to soil dust surfaces may also contribute to bio-INPs, leading to the high N_{INP} accompanied by high WS and Ca^{2+} .

However, we did observe that $N_{\text{INP-other org}}$ and $N_{\text{INP-inorg}}$ each exhibited positive correlations with temperature and negative correlations with WS, indicating that these particles have local sources. $N_{\text{INP-other org}}$ showed a positive correlation
295 with isoprene, which is considered to be an important natural gaseous precursor to the formation of secondary organic aerosols. Additionally, $N_{\text{INP-other org}}$ was positively correlated with the oxidation of isoprene bio-INPs, although this correlation was not significant. We hypothesize that the formation of secondary organic aerosols was the main source of other org-INPs.

$N_{\text{INP-inorg}}$ showed a positive correlation with BC in the LTR, but no significant correlation with inorganic ions (SNA and
300 Cl^-). BC-containing particles resulting from anthropogenic activities have been speculated to play a role in INPs formation (Kanji et al., 2017). However, aging processes, such as the coating of BC particles by SNA, may result in weakened heterogeneous ice nucleation activity of BC particles (Kulkarni et al., 2016). Our sampling site was relatively uninfluenced by anthropogenic activities, and previous studies based on high-altitude sites, such as Jungfraujoch (Hammer et al., 2018), also showed a weak activity of BC in ice formation.

305 **3.4 Transport pathways of INPs**

At the mountaintop site, the horizontal and vertical transport of air mass are important pathways for INPs under favorable conditions, such as valley breezes, variations in mixing layer height, and long-range transport processes. Understanding the coupling between the PBL changes and the air mass transport process can help us comprehend the characteristics of the target aerosols. Therefore, we conducted further analysis to examine the relationship between the PBL
310 height and N_{INP} , and combined it with CWT analysis to explore the effect of transport on INPs at the sampling site.

At Changbai Mountain, changes in the PBL are also complicated by a variety of processes, such as orographic gravity waves, moist convection, and turbulent transport. Figure 5(a–c) shows the relationship between bio-INPs and the PBL height



during the daytime. We found a moderate-to-good correlation between the PBL height and $N_{\text{INP-bio}}$ in the HTR ranging from $-12\text{ }^{\circ}\text{C}$ to $-10\text{ }^{\circ}\text{C}$, with r values between 0.4 and 0.7 (Figure 5a). Notably, this correlation was confined within the samples with low $N_{\text{INP-bio}}$ values, and we excluded two outliers with exceptionally high $N_{\text{INP-bio}}$ values. Our findings suggest that an increase in the PBL height may cause a corresponding increase in $N_{\text{INP-bio}}$ in the clean mountaintop atmosphere. Moreover, based on the analysis of the air mass backward trajectory, our analysis revealed a significant increase in the height of the air mass backward trajectory as it moved through the southwestern mountainous regions. This phenomenon indicates that valley breezes promote the lifting of INPs from the bottom to the top of Changbai Mountain during the daytime. However, the correlation between the PBL height and $N_{\text{INP-bio}}$ was no longer observed when the temperature dropped below $-13\text{ }^{\circ}\text{C}$ ($r < 0.4$, Figure 5c), indicating that the variation in the PBL did not significantly affect the ice nucleation of bio-INPs in the LTR.

Two high-value $N_{\text{INP-bio}}$ events occurred on August 18 and 25, 2021, with $N_{\text{INP-bio}}$ values approximately 12 times higher than during the remaining days. On August 18, 2021, the air mass originated from the Japan Sea and climbed to the sampling site from the southeastern hillside. However, on August 25, 2021, the air mass was primarily transported from South Korea over long distances in the troposphere. The CWT analysis revealed the potential sources of bio-INPs, as shown in Figure 5(d–f). The Japan Sea was identified as an important INPs source, as previous studies have reported that bubble bursting processes can release marine microorganisms (Burrows et al., 2013; Kwak et al., 2014; McCluskey et al., 2018; Vergara-Temprado et al., 2017). As phytoplankton blooms frequently occurred during our sampling period, it is possible that the air mass passing across the Japan Sea surface might have carried marine bio-INPs, contributing to their presence at the sampling site. Additionally, South Korea has a large vegetation coverage area, as shown in Figure 1(a), with biological aerosols produced there able to reach our sampling site through long-distance transport.

The residence time of various biological particles in the atmosphere can range from less than a day to a few weeks, depending on their size and aerodynamic properties (Despres et al., 2012). The long-range transport of biological aerosols has been observed in previous studies. For example, abundant microbial components originating from the ocean or land have been found in the troposphere, even extending to the stratosphere and the middle layer (Burrows et al., 2009; Smith et al., 2013). High concentrations of microbial populations have also been identified in the background atmosphere during trans-Pacific intercontinental transport (Smith et al., 2013). In global transmission, microorganisms have been found to travel thousands of kilometers, with approximately 33%–68% originating in the ocean. This suggests that the ocean's bubble bursting processes play a significant role in the generation of biological aerosols. In addition, bio-INPs can attach to dust particles for long-distance transmission, with an adhesion rate that can even exceed 99.9% (Creamean et al., 2013; Yahya et al., 2019). This process can enable biological aerosol transmission over longer distances, with the ice nucleation activity of dust significantly enhanced (O'sullivan et al., 2016; Augustin-Bauditz et al., 2016). Notably, the above discussion in this study does not include the qualitative and quantitative analyses of biological particles with ice-nucleating activity. Although long-range transported bio-INPs were less prominent in our study, their contribution to the total INPs concentration in the background atmosphere of northeastern Asia cannot be ignored.



In addition, a positive correlation was found between the PBL height and other org-INPs at temperatures ranging from $-19\text{ }^{\circ}\text{C}$ to $-13.5\text{ }^{\circ}\text{C}$ ($r = 0.5\text{--}0.8$) during the daytime, with significant correlations observed between $-18\text{ }^{\circ}\text{C}$ and $-17\text{ }^{\circ}\text{C}$, as shown in Figure S1. However, when the freezing temperatures dropped to below $-19.5\text{ }^{\circ}\text{C}$, no correlation was observed between the PBL and $N_{\text{INP-other org}}$, suggesting that local sources may be an important source for other org-INPs. The CWT simulation also indicated that high values of $N_{\text{INP-other org}}$ appeared in both local areas and adjacent Japan Sea regions (See Figure S2). For the inorg-INPs, a moderate correlation with the PBL height was observed at temperatures ranging from $-23\text{ }^{\circ}\text{C}$ to $-16\text{ }^{\circ}\text{C}$, but this was not statistically significant ($p > 0.05$). Compared with the bio-INPs and other org-INPs, we found that the contribution of local sources to the inorg-INPs significantly increased, while the contribution from oceanic sources greatly decreased.

In summary, our findings suggest that valley breezes influence the diurnal cycles of bio-INPs at Changbai Mountain, while the long-distance transport of air mass from the Japan Sea and South Korea significantly contributes to the high value of bio-INPs. However, the impact of the PBL and valley breezes on the transportation of other org-INPs and inorg-INPs was found to be less significant than the contributions of bio-INPs.

4 Conclusion

Measurements of INPs were carried out at the Changbai Mountain in northeastern Asia to explore the properties of INPs in the immersion freezing mode. Our results showed that N_{INP} spanned up to three orders of magnitude between $3.8 \times 10^{-3}\text{ L}^{-1}$ and 2.3 L^{-1} over the freezing temperature range from $-20.5\text{ }^{\circ}\text{C}$ to $-5.5\text{ }^{\circ}\text{C}$, with these values corresponding to previously reported measurements for mountain sites.

The INPs that we observed primarily consisted of protein-based bio-INPs. $F_{\text{INP-bio}}$ accounted for 100% of N_{INP} above $-11\text{ }^{\circ}\text{C}$, while showing a decreasing trend as the temperature decreased from $-11.5\text{ }^{\circ}\text{C}$ to $-16.5\text{ }^{\circ}\text{C}$. The decreasing trend of $F_{\text{INP-bio}}$ suggested that the ice nucleation activity of bio-INPs decreases with temperature. However, $F_{\text{INP-bio}}$ increased from 0.8 to 0.9 as the temperature decreased from $-16.5\text{ }^{\circ}\text{C}$ to $-20.0\text{ }^{\circ}\text{C}$, indicating that INPs have relatively high ice-nucleating activity in the LTR. We also found a significant positive correlation between biological INPs and both WS and Ca^{2+} , whereas there was only a weak positive correlation for biological INPs with isoprene and its oxidation products (isoprene \times O_3). We speculate that the higher WS may facilitate the exposure of the local soil dust and bioaerosols containing bio-INPs to the atmosphere.

At relatively high freezing temperatures, an increase in the PBL may cause a corresponding increase in $N_{\text{INP-bio}}$ in the clean mountaintop atmosphere. During the daytime, valley breezes facilitate the orographic lifting of INPs from the bottom to the top of southwestern mountainous regions. However, the high values of $N_{\text{INP-bio}}$ may originate from long-distance transport from the Japan Sea and South Korea areas. We speculate that the oceanic and vegetation biogenic aerosols from these areas make significant contributions to the INPs at the top of the Changbai Mountain. Conversely, regional transport



had a weaker effect on other org-INPs and inorg-INPs than bio-INPs, with larger contributions observed from local and oceanic sources.

380 The concentration of bio-INPs in the ambient atmosphere is typically lower than that found in ice crystals within clouds (Field et al., 2017). When measuring the ice crystals in clouds, biological sources can account for up to 33%, which is second only to the contribution of mineral dust (Murray et al., 2012). This suggests that primary bio-INPs triggering ice crystal formation alone cannot fully explain cloud observations, and that secondary ice formation, which involves the multiplication of ice crystal concentrations through various collisions with pre-existing ice (Qu et al., 2022), plays an important role. Our measurements in the high-altitude atmosphere above Northeast Asia confirm the predominant role of
385 bio-INPs, which can substantially impact ice crystals through both primary and secondary ice formation. However, due to the limited sample size, our results could not provide a comprehensive understanding of the characteristics of INPs in the high-altitude region. Further observational and modeling studies are urgently needed to analyze the characteristics of INPs and their influence on ice crystal formation as well as the cloud properties in the high-altitude atmosphere.

390 *Author contributions.* Yue Sun analyzed data and wrote the paper. Likun Xue designed the research. Jiangshan Mu, Ye Shan, Mingxuan Liu, Yanbin Qi, Lingli Zhang and Yufei Wang conducted the field campaign. Lanxiadi Chen and Mingjin Tang provided guidance and assistance in the analysis of INPs samples. Yu Yang, Yanqiu Nie, Ping Liu, Can Cui and Ji Zhang helped with the interpretation of the results. Yujiao Zhu, Likun Xue, Xinfeng Wang and Wenxing Wang revised the original manuscript. All authors contributed toward improving the paper.

395 *Competing interests.* The authors declare that they have no conflict of interest.

Data availability. The datasets related to this work can be accessed via <https://doi.org/10.17632/b9y6pfw39n.1> (Sun et al., 2023).

400 *Acknowledgements.* This work was funded by the National Natural Science Foundation of China (42075104, 41922051, 42061160478). We are grateful to the staff of the Tianchi weather station for their logistical support and assistance during the field observations. We would also like to acknowledge the Global Data Assimilation System (GDAS) provided by the National Oceanic and Atmospheric Administration Air Resources Laboratory (NOAA ARL) for organizing and
405 publishing the data, and the open-source software of MeteoInfo developed by Yaqiang Wang's team for the concentration-weighted trajectory (CWT) analysis.



References

- Agresti, A. and Coull, B. A.: Approximate is better than "exact" for interval estimation of binomial proportions, *Am. Stat.*,
410 52, 119-126, <https://doi.org/10.2307/2685469>, 1998.
- Alpert, P. A., Kilthau, W. P., O'Brien, R. E., Moffet, R. C., Gilles, M. K., Wang, B., Laskin, A., Aller, J. Y., and Knopf, D.
A.: Ice-nucleating agents in sea spray aerosol identified and quantified with a holistic multimodal freezing model, *Sci
Adv*, 8, <https://doi.org/10.1126/sciadv.abq6842>, 2022.
- Atkinson, J. D., Murray, B. J., Woodhouse, M. T., Whale, T. F., Baustian, K. J., Carslaw, K. S., Dobbie, S., O'Sullivan, D.,
415 and Malkin, T. L.: The importance of feldspar for ice nucleation by mineral dust in mixed-phase clouds, *Nature*, 498,
355-358, <https://doi.org/10.1038/nature12278>, 2013.
- Augustin-Bauditz, S., Wex, H., Denjean, C., Hartmann, S., Schneider, J., Schmidt, S., Ebert, M., and Stratmann, F.:
Laboratory-generated mixtures of mineral dust particles with biological substances: characterization of the particle
mixing state and immersion freezing behavior, *Atmos. Chem. Phys.*, 16, 5531-5543, <https://doi.org/10.5194/acp-16-5531-2016>, 2016.
420
- Beall, C. M., Hill, T. C. J., DeMott, P. J., Köneman, T., Pikridas, M., Drewnick, F., Harder, H., Pöhlker, C., Lelieveld, J.,
Weber, B., Iakovides, M., Prokeš, R., Sciare, J., Andreae, M. O., Stokes, M. D., and Prather, K. A.: Ice-nucleating
particles near two major dust source regions, *Atmos Chem Phys*, 22, 12607-12627, <https://doi.org/10.5194/acp-22-12607-2022>, 2022.
- 425 Bjordal, J., Storelvmo, T., Alterskjær, K., and Carlsen, T.: Equilibrium climate sensitivity above 5 °C plausible due to state-
dependent cloud feedback, *Nature Geoscience*, 13, 718-721, <https://doi.org/10.1038/s41561-020-00649-1>, 2020.
- Burrows, S. M., Elbert, W., Lawrence, M. G., and Pöschl, U.: Bacteria in the global atmosphere – Part 1: Review and
synthesis of literature data for different ecosystems, *Atmos. Chem. Phys.*, 9, 9263-9280, <https://doi.org/10.5194/acp-9-9263-2009>, 2009.
- 430 Burrows, S. M., Hoose, C., Pöschl, U., and Lawrence, M. G.: Ice nuclei in marine air: biogenic particles or dust?, *Atmos
Chem Phys*, 13, 245-267, [10.5194/acp-13-245-2013](https://doi.org/10.5194/acp-13-245-2013), 2013.
- Chen, J., Wu, Z., Chen, J., Reicher, N., Fang, X., Rudich, Y., and Hu, M.: Size-resolved atmospheric ice-nucleating particles
during East Asian dust events, *Atmos Chem Phys*, 21, 3491-3506, <https://doi.org/10.5194/acp-21-3491-2021>, 2021.
- Chen, J., Wu, Z., Augustin-Bauditz, S., Grawe, S., Hartmann, M., Pei, X., Liu, Z., Ji, D., and Wex, H.: Ice-nucleating
435 particle concentrations unaffected by urban air pollution in Beijing, China, *Atmos Chem Phys*, 18, 3523-3539,
<https://doi.org/10.5194/acp-18-3523-2018>, 2018.
- Chen, L., Peng, C., Chen, J., Chen, J., Gu, W., Jia, X., Wu, Z., Wang, Q., and Tang, M.: Effects of heterogeneous reaction
with NO₂ on ice nucleation activities of feldspar and Arizona Test Dust, *J Environ Sci-China*, 127, 210-221,
<https://doi.org/10.1016/j.jes.2022.04.034>, 2023.



- 440 Conen, F., Yakutin, M. V., Yttri, K. E., and Hüglin, C.: Ice Nucleating Particle Concentrations Increase When Leaves Fall in Autumn, *Atmosphere-Basel*, 8, 202, <https://doi.org/10.3390/atmos8100202>, 2017.
- Creamean, J. M., Suski, K. J., Rosenfeld, D., Cazorla, A., DeMott, P. J., Sullivan, R. C., White, A. B., Ralph, F. M., Minnis, P., Comstock, J. M., Tomlinson, J. M., and Prather, K. A.: Dust and Biological Aerosols from the Sahara and Asia Influence Precipitation in the Western U.S, *Science*, 339, 1572-1578, <https://doi.org/10.1126/science.1227279>, 2013.
- 445 Cziczo, D. J., Froyd, K. D., Gallavardin, S. J., Moehler, O., Benz, S., Saathoff, H., and Murphy, D. M.: Deactivation of ice nuclei due to atmospherically relevant surface coatings, *Environ Res Lett*, 4, 9, <https://doi.org/10.1088/1748-9326/4/4/044013>, 2009.
- Cziczo, D. J., Froyd, K. D., Hoose, C., Jensen, E. J., Diao, M. H., Zondlo, M. A., Smith, J. B., Twohy, C. H., and Murphy, D. M.: Clarifying the Dominant Sources and Mechanisms of Cirrus Cloud Formation, *Science*, 340, 1320-1324, <https://doi.org/10.1126/science.1234145>, 2013.
- 450 Daily, M. I., Tarn, M. D., Whale, T. F., and Murray, B. J.: An evaluation of the heat test for the ice-nucleating ability of minerals and biological material, *Atmos. Meas. Tech.*, 15, 2635-2665, <https://doi.org/10.5194/amt-15-2635-2022>, 2022.
- Demott, P. J.: An Exploratory Study of Ice Nucleation by Soot Aerosols, *J Appl Meteorol*, 29, 1072-1079, [https://doi.org/10.1175/1520-0450\(1990\)029<1072:Aesoin>2.0.Co;2](https://doi.org/10.1175/1520-0450(1990)029<1072:Aesoin>2.0.Co;2), 1990.
- 455 DeMott, P. J., Cziczo, D. J., Prenni, A. J., Murphy, D. M., Kreidenweis, S. M., Thomson, D. S., Borys, R., and Rogers, D. C.: Measurements of the concentration and composition of nuclei for cirrus formation, *Proceedings of the National Academy of Sciences*, 100, 14655-14660, <https://doi.org/10.1073/pnas.2532677100>, 2003.
- DeMott, P. J., Prenni, A. J., Liu, X., Kreidenweis, S. M., Petters, M. D., Twohy, C. H., Richardson, M. S., Eidhammer, T., and Rogers, D. C.: Predicting global atmospheric ice nuclei distributions and their impacts on climate, *P Natl Acad Sci USA*, 107, 11217-11222, <https://doi.org/10.1073/pnas.0910818107>, 2010.
- 460 DeMott, P. J., Prenni, A. J., McMeeking, G. R., Sullivan, R. C., Petters, M. D., Tobo, Y., Niemand, M., Mohler, O., Snider, J. R., Wang, Z., and Kreidenweis, S. M.: Integrating laboratory and field data to quantify the immersion freezing ice nucleation activity of mineral dust particles, *Atmos Chem Phys*, 15, 393-409, <https://doi.org/10.5194/acp-15-393-2015>, 2015.
- 465 Despres, V. R., Huffman, J. A., Burrows, S. M., Hoose, C., Safatov, A. S., Buryak, G., Frohlich-Nowoisky, J., Elbert, W., Andreae, M. O., Poschl, U., and Jaenicke, R.: Primary biological aerosol particles in the atmosphere: a review, *Tellus B*, 64, 58, <https://doi.org/10.3402/tellusb.v64i0.15598>, 2012.
- Diehl, K. and Mitra, S. K.: A laboratory study of the effects of a kerosene-burner exhaust on ice nucleation and the evaporation rate of ice crystals, *Atmospheric Environment*, 32, 3145-3151, [https://doi.org/10.1016/s1352-2310\(97\)00467-6](https://doi.org/10.1016/s1352-2310(97)00467-6), 1998.
- 470 Field, P. R., Lawson, R. P., Brown, P. R. A., Lloyd, G., Westbrook, C., Moisseev, D., Miltenberger, A., Nenes, A., Blyth, A., Choularton, T., Connolly, P., Buehl, J., Crosier, J., Cui, Z., Dearden, C., DeMott, P., Flossmann, A., Heymsfield, A., Huang, Y., Kalesse, H., Kanji, Z. A., Korolev, A., Kirchgaessner, A., Lasher-Trapp, S., Leisner, T., McFarquhar, G.,



- 475 Phillips, V., Stith, J., and Sullivan, S.: Secondary Ice Production: Current State of the Science and Recommendations
for the Future, *Meteorological Monographs*, 58, 7.1-7.20, <https://doi.org/10.1175/AMSMONOGRAPHS-D-16-0014.1>,
2017.
- Fornea, A. P., Brooks, S. D., Dooley, J. B., and Saha, A.: Heterogeneous freezing of ice on atmospheric aerosols containing
ash, soot, and soil, *J Geophys Res-Atmos*, 114, 12, <https://doi.org/10.1029/2009jd011958>, 2009.
- 480 Freedman, M. A.: Potential Sites for Ice Nucleation on Aluminosilicate Clay Minerals and Related Materials, *J. Phys. Chem.*
Let., 6, 3850-3858, <https://doi.org/10.1021/acs.jpcclett.5b01326>, 2015.
- Gong, X., Radenz, M., Wex, H., Seifert, P., Ataei, F., Henning, S., Baars, H., Barja, B., Ansmann, A., and Stratmann, F.:
Significant continental source of ice-nucleating particles at the tip of Chile's southernmost Patagonia region, *Atmos*
Chem Phys, 22, 10505-10525, <https://doi.org/10.5194/acp-2022-71>, 2022.
- 485 Grawe, S., Augustin-Bauditz, S., Hartmann, S., Hellner, L., Pettersson, J. B. C., Prager, A., Stratmann, F., and Wex, H.: The
immersion freezing behavior of ash particles from wood and brown coal burning, *Atmos. Chem. Phys.*, 16, 13911-
13928, <https://doi.org/10.5194/acp-16-13911-2016>, 2016.
- Grawe, S., Augustin-Bauditz, S., Clemen, H. C., Ebert, M., Hammer, S. E., Lubitz, J., Reicher, N., Rudich, Y., Schneider, J.,
Staacke, R., Stratmann, F., Welti, A., and Wex, H.: Coal fly ash: linking immersion freezing behavior and
physicochemical particle properties, *Atmos Chem Phys*, 18, 13903-13923, <https://doi.org/10.5194/acp-18-13903-2018>,
490 2018.
- Hammer, S. E., Mertes, S., Schneider, J., Ebert, M., Kandler, K., and Weinbruch, S.: Composition of ice particle residuals in
mixed-phase clouds at Jungfraujoch (Switzerland): enrichment and depletion of particle groups relative to total aerosol,
Atmos Chem Phys, 18, 13987-14003, <https://doi.org/10.5194/acp-18-13987-2018>, 2018.
- 495 Harrison, A. D., Whale, T. F., Carpenter, M. A., Holden, M. A., Neve, L., O'Sullivan, D., Vergara Temprado, J., and Murray,
B. J.: Not all feldspars are equal: a survey of ice nucleating properties across the feldspar group of minerals, *Atmos.*
Chem. Phys., 16, 10927-10940, <https://doi.org/10.5194/acp-16-10927-2016>, 2016.
- Hoose, C. and Möhler, O.: Heterogeneous ice nucleation on atmospheric aerosols: a review of results from laboratory
experiments, *Atmos Chem Phys*, 12, 9817-9854, <https://doi.org/10.5194/acp-12-9817-2012>, 2012.
- 500 Huang, S., Hu, W., Chen, J., Wu, Z., Zhang, D., and Fu, P.: Overview of biological ice nucleating particles in the atmosphere,
Environment International, 146, 106197, <https://doi.org/10.1016/j.envint.2020.106197>, 2021.
- Hummel, M., Hoose, C., Pummer, B., Schaupp, C., Frohlich-Nowoisky, J., and Mohler, O.: Simulating the influence of
primary biological aerosol particles on clouds by heterogeneous ice nucleation, *Atmos Chem Phys*, 18, 15437-15450,
<https://doi.org/10.5194/acp-18-15437-2018>, 2018.
- 505 Iannone, R., Chernoff, D. I., Pringle, A., Martin, S. T., and Bertram, A. K.: The ice nucleation ability of one of the most
abundant types of fungal spores found in the atmosphere, *Atmos Chem Phys*, 11, 1191-1201,
<https://doi.org/10.5194/acp-11-1191-2011>, 2011.



- Jiang, H., Yin, Y., Su, H., Shan, Y. P., and Gao, R. J.: The characteristics of atmospheric ice nuclei measured at the top of Huangshan (the Yellow Mountains) in Southeast China using a newly built static vacuum water vapor diffusion chamber, *Atmos Res*, 153, 200-208, <https://doi.org/10.1016/j.atmosres.2014.08.015>, 2015.
- 510 Jiang, H., Yin, Y., Chen, K., Chen, Q., He, C., and Sun, L.: The measurement of ice nucleating particles at Tai'an city in East China, *Atmos Res*, 232, 9, <https://doi.org/10.1016/j.atmosres.2019.104684>, 2020.
- Jiang, H., Yin, Y., Yang, L., Yang, S. Z., Su, H., and Chen, K.: The Characteristics of Atmospheric Ice Nuclei Measured at Different Altitudes in the Huangshan Mountains in Southeast China, *Adv. Atmos. Sci.*, 31, 396-406, <https://doi.org/10.1007/s00376-013-3048-5>, 2014.
- 515 Jin, Y. H., Zhang, Y. J., Xu, J. W., Tao, Y., He, H. S., Guo, M., Wang, A. L., Liu, Y. X., and Niu, L. P.: Comparative Assessment of Tundra Vegetation Changes Between North and Southwest Slopes of Changbai Mountains, China, in Response to Global Warming, *Chin. Geogr. Sci.*, 28, 665-679, <https://doi.org/10.1007/s11769-018-0978-y>, 2018.
- Joly, M., Amato, P., Deguillaume, L., Monier, M., Hoose, C., and Delort, A. M.: Quantification of ice nuclei active at near 0 °C temperatures in low-altitude clouds at the Puy de Dôme atmospheric station, *Atmos. Chem. Phys.*, 14, 8185-8195, <https://doi.org/10.5194/acp-14-8185-2014>, 2014.
- 520 Jung, S., Tiwari, M. K., and Poulidakos, D.: Frost halos from supercooled water droplets, *P Natl Acad Sci USA*, 109, 16073-16078, <https://doi.org/10.1073/pnas.1206121109>, 2012.
- Kanji, Z. A. and Abbatt, J. P. D.: Ice Nucleation onto Arizona Test Dust at Cirrus Temperatures: Effect of Temperature and Aerosol Size on Onset Relative Humidity, *J Phys Chem A*, 114, 935-941, <https://doi.org/10.1021/jp908661m>, 2010.
- 525 Kanji, Z. A., Ladino, L. A., Wex, H., Boose, Y., Burkert-Kohn, M., Cziczo, D. J., and Krämer, M.: Overview of Ice Nucleating Particles, *Meteorological Monographs*, 58, 1.1-1.33, <https://doi.org/10.1175/amsmonographs-d-16-0006.1>, 2017.
- Knopf, D. A., Wang, B., Laskin, A., Moffet, R. C., and Gilles, M. K.: Heterogeneous nucleation of ice on anthropogenic organic particles collected in Mexico City, *Geophys Res Lett*, 37, 5, <https://doi.org/10.1029/2010gl043362>, 2010.
- 530 Koop, T., Luo, B., Tsias, A., and Peter, T.: Water activity as the determinant for homogeneous ice nucleation in aqueous solutions, *Nature*, 406, 611-614, <https://doi.org/10.1038/35020537>, 2000.
- Kulkarni, G., China, S., Liu, S., Nandasiri, M., Sharma, N., Wilson, J., Aiken, A. C., Chand, D., Laskin, A., Mazzoleni, C., Pekour, M., Shilling, J., Shutthanandan, V., Zelenyuk, A., and Zaveri, R. A.: Ice nucleation activity of diesel soot particles at cirrus relevant temperature conditions: Effects of hydration, secondary organics coating, soot morphology, and coagulation, *Geophys Res Lett*, 43, 3580-3588, <https://doi.org/10.1002/2016GL068707>, 2016.
- 535 Kwak, J. H., Lee, S. H., Hwang, J., Suh, Y. S., Park, H. J., Chang, K. I., Kim, K. R., and Kang, C. K.: Summer primary productivity and phytoplankton community composition driven by different hydrographic structures in the East/Japan Sea and the Western Subarctic Pacific, *J. Geophys. Res.-Oceans*, 119, 4505-4519, <https://doi.org/10.1002/2014jc009874>, 2014.



- 540 Lu, Z. D., Du, P. R., Du, R., Liang, Z. M., Qin, S. S., Li, Z. M., and Wang, Y. L.: The Diversity and Role of Bacterial Ice Nuclei in Rainwater from Mountain Sites in China, *Aerosol Air Qual Res*, 16, 640-652, <https://doi.org/10.4209/aaqr.2015.05.0315>, 2016.
- Mahrt, F., Marcolli, C., David, R. O., Gronquist, P., Meier, E. J. B., Lohmann, U., and Kanji, Z. A.: Ice nucleation abilities of soot particles determined with the Horizontal Ice Nucleation Chamber, *Atmos Chem Phys*, 18, 13363-13392, <https://doi.org/10.5194/acp-18-13363-2018>, 2018.
- 545 Maki, L. R., Galyan, E. L., Changchi, M., and Caldwell, D. R.: Ice Nucleation Induced by *Pseudomonas syringae*, *Applied Microbiology*, 28, 456-459, <https://doi.org/10.1128/aem.28.3.456-459.1974>, 1974.
- McCluskey, C. S., Hill, T. C. J., Malfatti, F., Sultana, C. M., Lee, C., Santander, M. V., Beall, C. M., Moore, K. A., Cornwell, G. C., Collins, D. B., Prather, K. A., Jayarathne, T., Stone, E. A., Azam, F., Kreidenweis, S. M., and DeMott, P. J.: A
550 Dynamic Link between Ice Nucleating Particles Released in Nascent Sea Spray Aerosol and Oceanic Biological Activity during Two Mesocosm Experiments, *J Atmos Sci*, 74, 151-166, [10.1175/jas-d-16-0087.1](https://doi.org/10.1175/jas-d-16-0087.1), 2017.
- McCluskey, C. S., Ovadnevaite, J., Rinaldi, M., Atkinson, J., Belosi, F., Ceburnis, D., Marullo, S., Hill, T. C. J., Lohmann, U., Kanji, Z. A., O'Dowd, C., Kreidenweis, S. M., and DeMott, P. J.: Marine and Terrestrial Organic Ice-Nucleating
555 Particles in Pristine Marine to Continentally Influenced Northeast Atlantic Air Masses, *J Geophys Res-Atmos*, 123, 6196-6212, <https://doi.org/10.1029/2017jd028033>, 2018.
- Moffett, B. F., Getti, G., Henderson-Begg, S. K., and Hill, T. C. J.: Ubiquity of ice nucleation in lichen — possible atmospheric implications, *Lindbergia*, 3, 39-43, <https://doi.org/10.25227/linbg.01070>, 2015.
- Murray, B. J., O'Sullivan, D., Atkinson, J. D., and Webb, M. E.: Ice nucleation by particles immersed in supercooled cloud droplets, *Chem. Soc. Rev.*, 41, 6519-6554, <https://doi.org/10.1039/c2cs35200a>, 2012.
- 560 Murray, B. J., Broadley, S. L., Wilson, T. W., Bull, S. J., Wills, R. H., Christenson, H. K., and Murray, E. J.: Kinetics of the homogeneous freezing of water, *Phys Chem Chem Phys*, 12, 10380-10387, <https://doi.org/10.1039/C003297B>, 2010.
- Nichman, L., Wolf, M., Davidovits, P., Onasch, T. B., Zhang, Y., Worsnop, D. R., Bhandari, J., Mazzoleni, C., and Cziczo, D. J.: Laboratory study of the heterogeneous ice nucleation on black-carbon-containing aerosol, *Atmos. Chem. Phys.*, 19, 12175-12194, <https://doi.org/10.5194/acp-19-12175-2019>, 2019.
- 565 O'Sullivan, D., Murray, B. J., Ross, J. F., and Webb, M. E.: The adsorption of fungal ice-nucleating proteins on mineral dusts: a terrestrial reservoir of atmospheric ice-nucleating particles, *Atmos. Chem. Phys.*, 16, 7879-7887, <https://doi.org/10.5194/acp-16-7879-2016>, 2016.
- O'Sullivan, D., Adams, M. P., Tarn, M. D., Harrison, A. D., Vergara-Temprado, J., Porter, G. C. E., Holden, M. A., Sanchez-Marroquin, A., Carotenuto, F., Whale, T. F., McQuaid, J. B., Walshaw, R., Hedges, D. H. P., Burke, I. T., Cui, Z., and Murray, B. J.: Contributions of biogenic material to the atmospheric ice-nucleating particle population in North
570 Western Europe, *Sci Rep*, 8, 13821, <https://doi.org/10.1038/s41598-018-31981-7>, 2018.
- Petters, M. D. and Wright, T. P.: Revisiting ice nucleation from precipitation samples, *Geophys Res Lett*, 42, 8758-8766, <https://doi.org/10.1002/2015GL065733>, 2015.



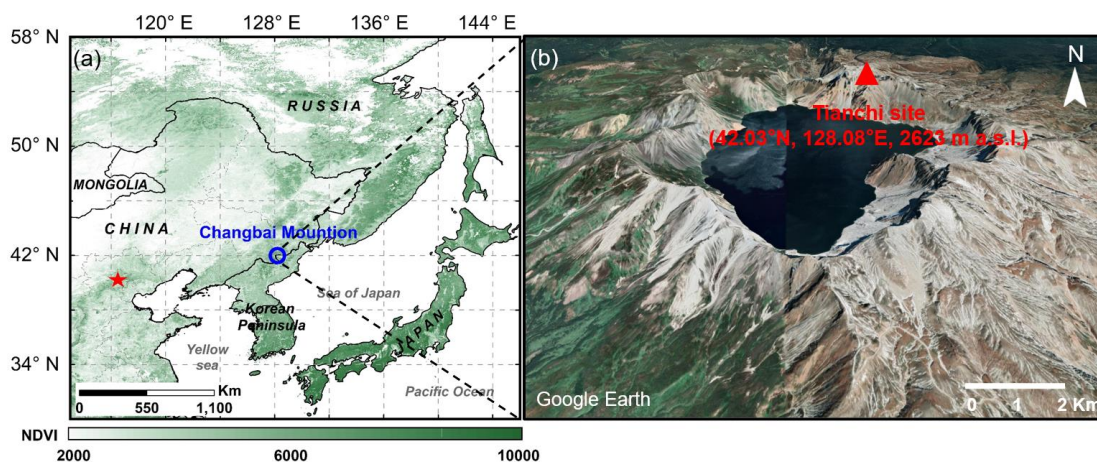
- Phillips, V. T. J., Donner, L. J., and Garner, S. T.: Nucleation Processes in Deep Convection Simulated by a Cloud-System-
575 Resolving Model with Double-Moment Bulk Microphysics, *J Atmos Sci*, 64, 738-761, <https://doi.org/10.1175/jas3869.1>, 2007.
- Pratt, K. A., DeMott, P. J., French, J. R., Wang, Z., Westphal, D. L., Heymsfield, A. J., Twohy, C. H., Prenni, A. J., and
Prather, K. A.: In situ detection of biological particles in cloud ice-crystals, *Nature Geoscience*, 2, 397-400,
<https://doi.org/10.1038/ngeo521>, 2009.
- 580 Pummer, B. G., Bauer, H., Bernardi, J., Bleicher, S., and Grothe, H.: Suspendable macromolecules are responsible for ice
nucleation activity of birch and conifer pollen, *Atmos Chem Phys*, 12, 2541-2550, [https://doi.org/10.5194/acp-12-2541-](https://doi.org/10.5194/acp-12-2541-2012)
2012, 2012.
- Qu, Z., Korolev, A., Milbrandt, J. A., Heckman, I., Huang, Y., McFarquhar, G. M., Morrison, H., Wolde, M., and Nguyen,
C.: The impacts of secondary ice production on microphysics and dynamics in tropical convection, *Atmos. Chem. Phys.*,
585 22, 12287-12310, <https://doi.org/10.5194/acp-22-12287-2022>, 2022.
- Rinaldi, M., Santachiara, G., Nicosia, A., Piazza, M., Decesari, S., Gilardoni, S., Paglione, M., Cristofanelli, P., Marinoni, A.,
Bonasoni, P., and Belosi, F.: Atmospheric Ice Nucleating Particle measurements at the high mountain observatory Mt.
Cimone (2165 m a.s.l., Italy), *Atmospheric Environment*, 171, 173-180, <https://doi.org/10.1016/j.atmosenv.2017.10.027>,
2017.
- 590 Rosenfeld, D. and Woodley, W. L.: Deep convective clouds with sustained supercooled liquid water down to - 37.5 °C,
Nature, 405, 440-442, <https://doi.org/10.1038/35013030>, 2000.
- Roudsari, G., Pakarinen, O. H., Reischl, B., and Vehkamäki, H.: Atomistic and coarse-grained simulations reveal increased
ice nucleation activity on silver iodide surfaces in slit and wedge geometries, *Atmos. Chem. Phys.*, 22, 10099-10114,
<https://doi.org/10.5194/acp-22-10099-2022>, 2022.
- 595 Sassen, K. and Khvorostyanov, V. I.: Cloud effects from boreal forest fire smoke: evidence for ice nucleation from
polarization lidar data and cloud model simulations, *Environ Res Lett*, 3, 12, [https://doi.org/10.1088/1748-](https://doi.org/10.1088/1748-9326/3/2/025006)
9326/3/2/025006, 2008.
- Schill, G. P., DeMott, P. J., Emerson, E. W., Rauker, A. M. C., Kodros, J. K., Suski, K. J., Hill, T. C. J., Levin, E. J. T.,
Pierce, J. R., Farmer, D. K., and Kreidenweis, S. M.: The contribution of black carbon to global ice nucleating particle
600 concentrations relevant to mixed-phase clouds, *P Natl Acad Sci USA*, 117, 22705-22711,
<https://doi.org/10.1073/pnas.2001674117>, 2020.
- Schrod, J., Weber, D., Drucke, J., Keleshis, C., Pikridas, M., Ebert, M., Cvetkovic, B., Nickovic, S., Marinou, E., Baars, H.,
Ansmann, A., Vrekoussis, M., Mihalopoulos, N., Sciare, J., Curtius, J., and Bingemer, H. G.: Ice nucleating particles
over the Eastern Mediterranean measured by unmanned aircraft systems, *Atmos Chem Phys*, 17, 4817-4835,
605 <https://doi.org/10.5194/acp-17-4817-2017>, 2017.



- Smith, D. J., Timonen, H. J., Jaffe, D. A., Griffin, D. W., Birmele, M. N., Perry, K. D., Ward, P. D., and Roberts, M. S.: Intercontinental Dispersal of Bacteria and Archaea by Transpacific Winds, *Appl. Environ. Microbiol.*, 79, 1134-1139, <https://doi.org/10.1128/AEM.03029-12>, 2013.
- Stein, A. F., Draxler, R. R., Rolph, G. D., Stunder, B. J. B., Cohen, M. D., and Ngan, F.: NOAA's HYSPLIT Atmospheric Transport and Dispersion Modeling System, *Bulletin of the American Meteorological Society*, 96, 2059-2077, <https://doi.org/10.1175/bams-d-14-00110.1>, 2015.
- Sugita, M., Asanuma, J., Tsujimura, M., Mariko, S., Lu, M., Kimura, F., Azzaya, D., and Adyasuren, T.: An overview of the rangelands atmosphere–hydrosphere–biosphere interaction study experiment in northeastern Asia (RAISE), *J Hydrol*, 333, 3-20, <https://doi.org/10.1016/j.jhydrol.2006.07.032>, 2007.
- Suski, K. J., Hill, T. C. J., Levin, E. J. T., Miller, A., DeMott, P. J., and Kreidenweis, S. M.: Agricultural harvesting emissions of ice-nucleating particles, *Atmos. Chem. Phys.*, 18, 13755-13771, <https://doi.org/10.5194/acp-18-13755-2018>, 2018.
- Tang, M. J., Chen, J., and Wu, Z.: Ice nucleating particles in the troposphere: Progresses, challenges and opportunities, *Atmospheric Environment*, 192, 206-208, <https://doi.org/10.1016/j.atmosenv.2018.09.004>, 2018.
- Tang, M. J., Cziczo, D. J., and Grassian, V. H.: Interactions of Water with Mineral Dust Aerosol: Water Adsorption, Hygroscopicity, Cloud Condensation, and Ice Nucleation, *Chem Rev*, 116, 4205-4259, <https://doi.org/10.1021/acs.chemrev.5b00529>, 2016.
- Testa, B., Hill, T. C. J., Marsden, N. A., Barry, K. R., Hume, C. C., Bian, Q. J., Uetake, J., Hare, H., Perkins, R. J., Mohler, O., Kreidenweis, S. M., and DeMott, P. J.: Ice Nucleating Particle Connections to Regional Argentinian Land Surface Emissions and Weather During the Cloud, Aerosol, and Complex Terrain Interactions Experiment, *J Geophys Res-Atmos*, 126, 26, <https://doi.org/10.1029/2021jd035186>, 2021.
- Tobo, Y., Prenni, A. J., DeMott, P. J., Huffman, J. A., McCluskey, C. S., Tian, G. X., Pohlker, C., Poschl, U., and Kreidenweis, S. M.: Biological aerosol particles as a key determinant of ice nuclei populations in a forest ecosystem, *J Geophys Res-Atmos*, 118, 10100-10110, <https://doi.org/10.1002/jgrd.50801>, 2013.
- Umo, N. S., Murray, B. J., Baeza-Romero, M. T., Jones, J. M., Lea-Langton, A. R., Malkin, T. L., O'Sullivan, D., Neve, L., Plane, J. M. C., and Williams, A.: Ice nucleation by combustion ash particles at conditions relevant to mixed-phase clouds, *Atmos. Chem. Phys.*, 15, 5195-5210, <https://doi.org/10.5194/acp-15-5195-2015>, 2015.
- Vali, G.: Quantitative Evaluation of Experimental Results on the Heterogeneous Freezing Nucleation of Supercooled Liquids, *Journal of Atmospheric Sciences*, 28, 402-409, [https://doi.org/10.1175/1520-0469\(1971\)028<0402:Qeoera>2.0.Co;2](https://doi.org/10.1175/1520-0469(1971)028<0402:Qeoera>2.0.Co;2), 1971.
- Vali, G., DeMott, P. J., Mohler, O., and Whale, T. F.: Technical Note: A proposal for ice nucleation terminology, *Atmos Chem Phys*, 15, 10263-10270, <https://doi.org/10.5194/acp-15-10263-2015>, 2015.
- Vergara-Temprado, J., Murray, B. J., Wilson, T. W., O'Sullivan, D., Browse, J., Pringle, K. J., Ardon-Dryer, K., Bertram, A. K., Burrows, S. M., Ceburnis, D., DeMott, P. J., Mason, R. H., O'Dowd, C. D., Rinaldi, M., and Carslaw, K. S.:



- 640 Contribution of feldspar and marine organic aerosols to global ice nucleating particle concentrations, *Atmos. Chem. Phys.*, 17, 3637-3658, <https://doi.org/10.5194/acp-17-3637-2017>, 2017.
- Welti, A., Müller, K., Fleming, Z. L., and Stratmann, F.: Concentration and variability of ice nuclei in the subtropical maritime boundary layer, *Atmos. Chem. Phys.*, 18, 5307-5320, [10.5194/acp-18-5307-2018](https://doi.org/10.5194/acp-18-5307-2018), 2018.
- Whale, T. F., Holden, M. A., Wilson, Theodore W., O'Sullivan, D., and Murray, B. J.: The enhancement and suppression of immersion mode heterogeneous ice-nucleation by solutes, *Chemical Science*, 9, 4142-4151, <https://doi.org/10.1039/C7SC05421A>, 2018.
- 645 Wieder, J., Mignani, C., Schär, M., Roth, L., Sprenger, M., Henneberger, J., Lohmann, U., Brunner, C., and Kanji, Z. A.: Unveiling atmospheric transport and mixing mechanisms of ice-nucleating particles over the Alps, *Atmos Chem Phys*, 22, 3111-3130, <https://doi.org/10.5194/acp-22-3111-2022>, 2022.
- 650 Yahya, R. Z., Arrieta, J. M., Cusack, M., and Duarte, C. M.: Airborne Prokaryote and Virus Abundance Over the Red Sea, *Front. Microbiol.*, 10, 10, <https://doi.org/10.3389/fmicb.2019.01112>, 2019.
- Zhang, P., Wu, Z., and Jin, R.: How can the winter North Atlantic Oscillation influence the early summer precipitation in Northeast Asia: effect of the Arctic sea ice, *Clim Dynam*, 56, 1989-2005, <https://doi.org/10.1007/s00382-020-05570-2>, 2021.
- 655 Zhou, C., Zelinka, M. D., and Klein, S. A.: Impact of decadal cloud variations on the Earth's energy budget, *Nature Geoscience*, 9, 871-874, <https://doi.org/10.1038/ngeo2828>, 2016.



660 **Figure 1. Geographical maps showing the location of Changbai Mountain. (a) This map is color-coded according to the normalized difference vegetation index (NDVI) in 2015, which was downloaded from the Geospatial Data Cloud (<https://www.gscloud.cn/search>). (b) This map shows the three-dimensional shape of the sampling site, which was obtained from © Google Earth.**



665

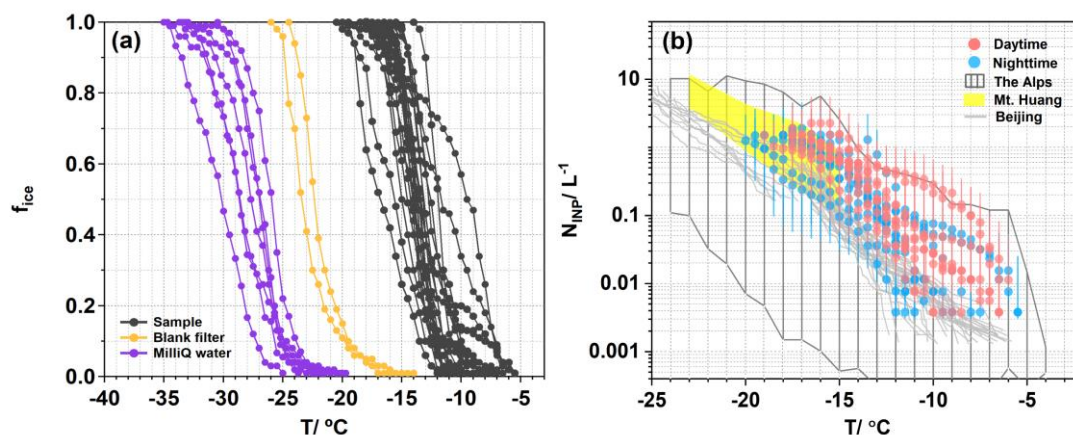


Figure 2. Frozen fractions (f_{ice}) and concentrations of INPs (N_{INP}) as functions of temperature. (a) The f_{ice} of collected samples measured by GIGINA is shown by the black curves, and presented together with blank filters (orange curves) and MilliQ water (purple curves) as background signals. (b) N_{INP} was measured during the daytime and nighttime, with error bars indicating the 95% confidence intervals. The dark gray shaded area represents the upper and lower limits of N_{INP} over the Alps (2693 m a.s.l.) (Wieder et al., 2022). The yellow shaded area represents the atmospheric N_{INP} ranges at Mt. Huang (1840 m a.s.l.) (Jiang et al., 2015). And the light gray lines represent N_{INP} in Beijing (Chen et al., 2018).

670

675

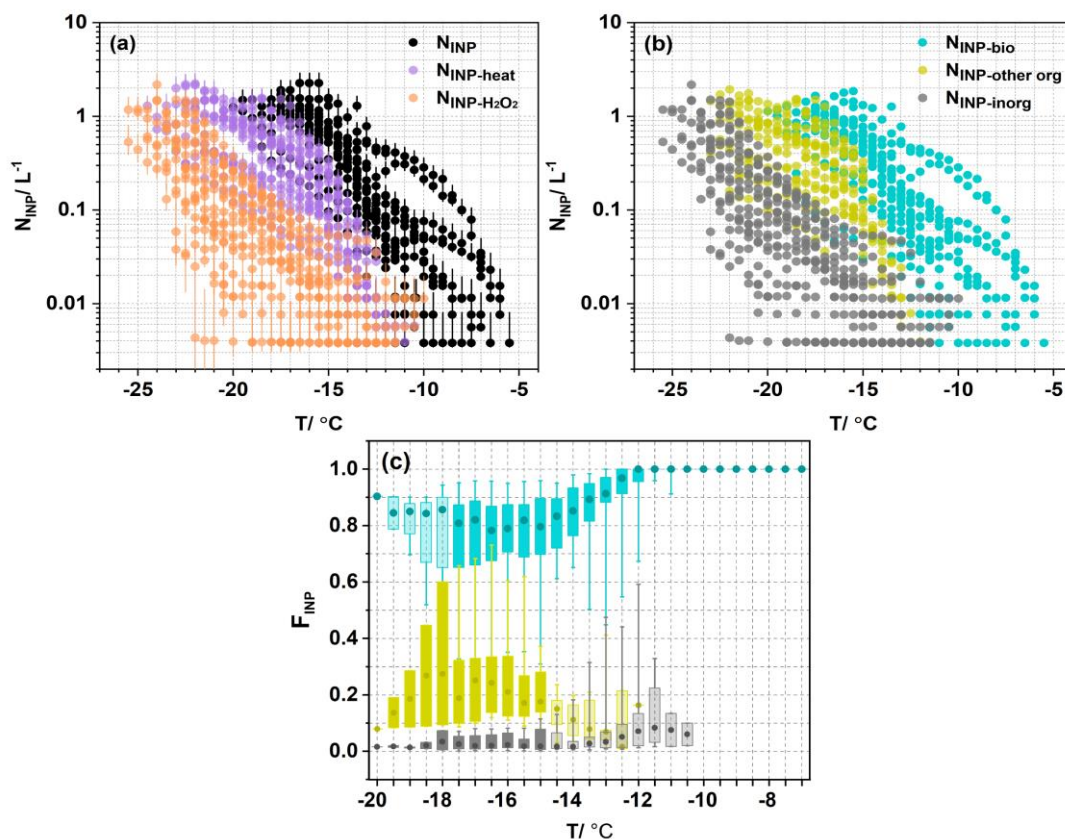


Figure 3. N_{INP} for different types of INPs and their fractions as functions of temperature. (a) The original N_{INP} is marked by black dots, $N_{\text{INP-heat}}$ is marked by purple dots, and $N_{\text{INP-H}_2\text{O}_2}$ is marked by pink dots, with 20% error bars indicating the 95% confidence intervals. (b) The INPs spectra of biological INPs ($N_{\text{INP-bio}}$, blue dots), other organic INPs ($N_{\text{INP-other org}}$, yellow dots), and inorganic INPs ($N_{\text{INP-inorg}}$, gray dots). (c) Boxplot of fractions of bio-INPs ($F_{\text{INP-bio}}$, blue boxplot), other org-INPs ($F_{\text{INP-other org}}$, yellow boxplot), and inorganic INPs ($F_{\text{INP-inorg}}$, gray boxplot) as functions of temperature. The upper and lower extents of the boxes represent the 75th and 25th percentiles, respectively, while the whiskers indicate the minimum and maximum values. The circle in each boxplot represents the median value. The light-colored boxes indicate that the number of data points is less than half of all samples at each temperature.

680

685

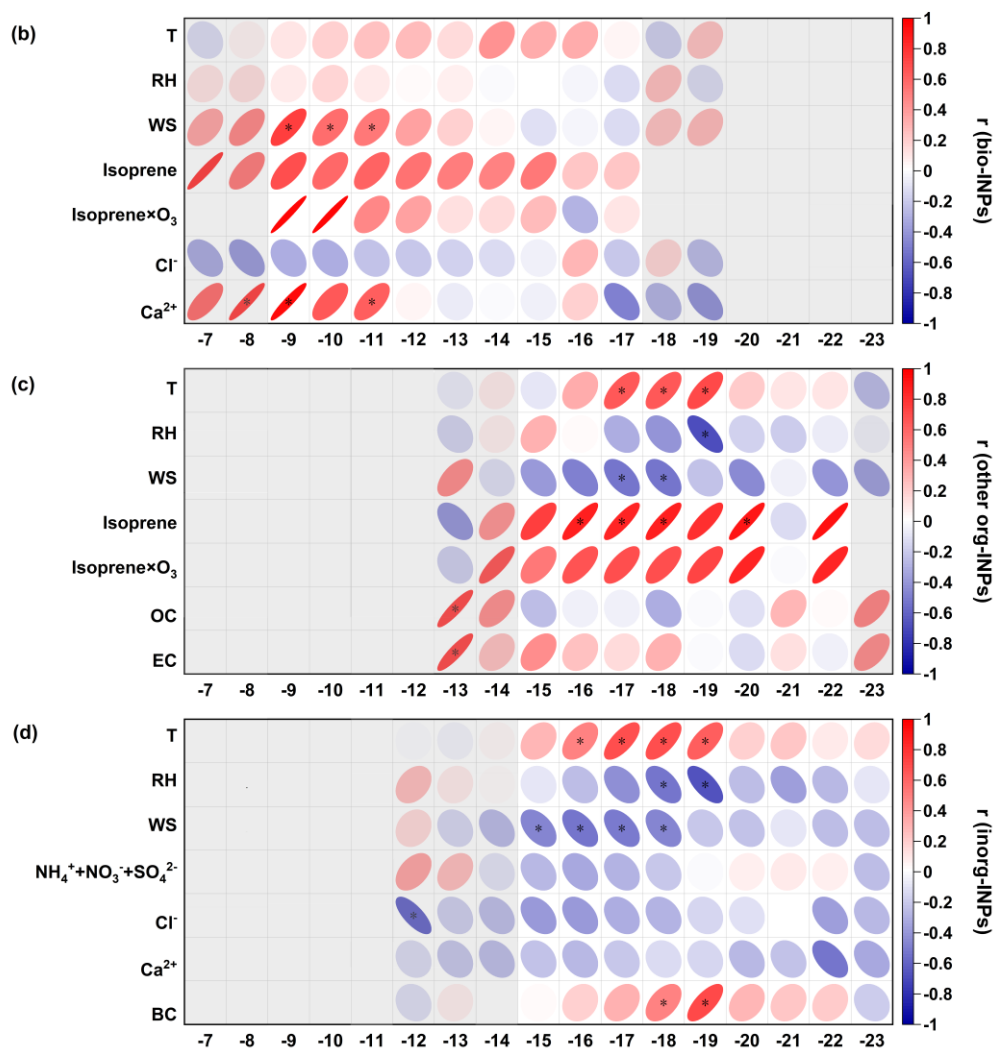
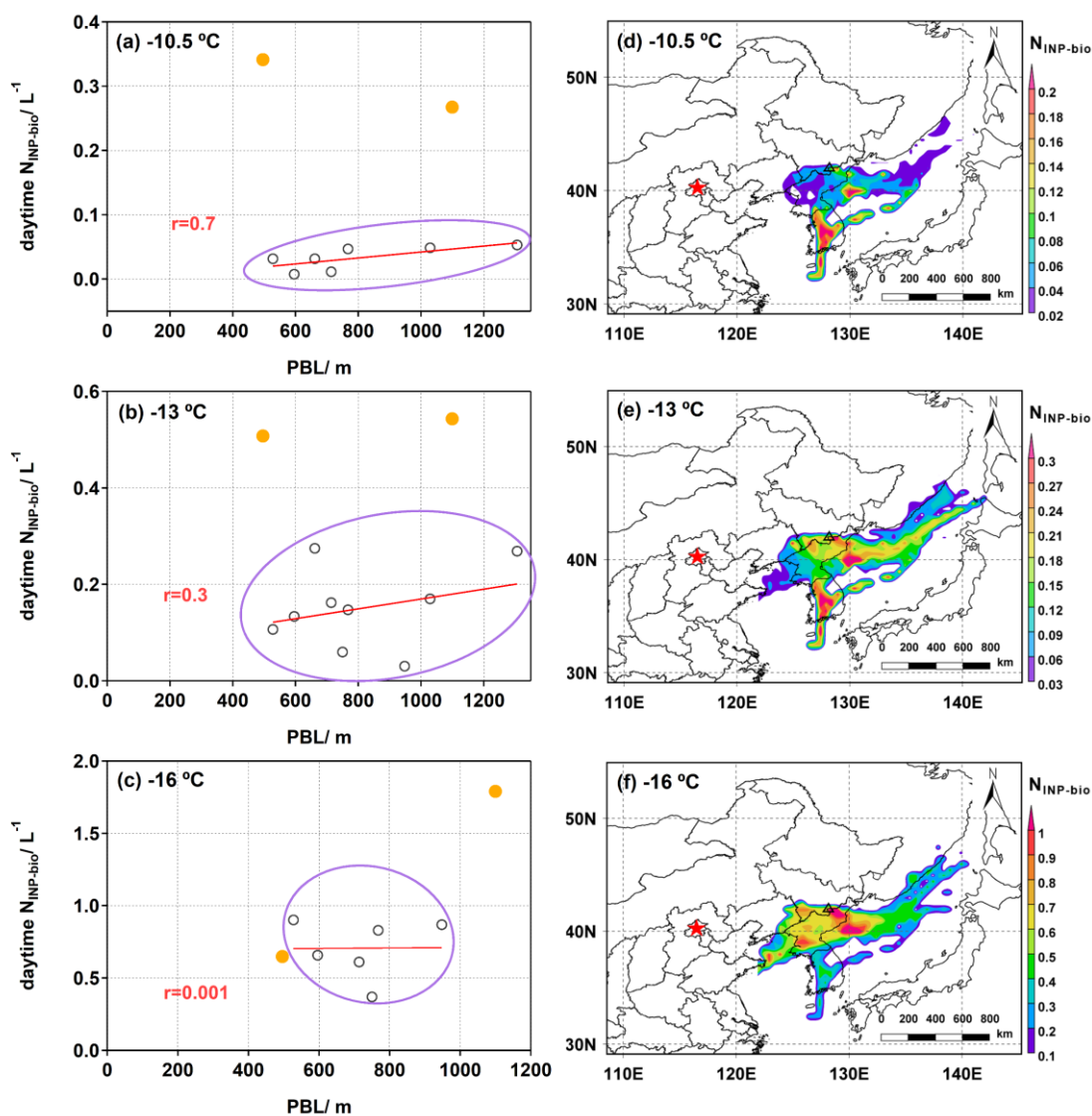


Figure 4. Correlation analysis between (a) N_{INP} , (b) N_{INP} -bio, (c) N_{INP} -other org, (d) N_{INP} -inorg, and meteorological parameters, chemical compositions, as functions of temperature. The asterisk indicates $p < 0.05$, while the shades indicate that the number of data points is less than half of all samples at each temperature.



695 **Figure 5. Relationship between $N_{\text{INP-bio}}$ and PBL height during the daytime (8:00–17:00, m above ground level) at three temperatures: (a) -10.5°C , (b) -13°C and (c) -16°C . Two outliers of $N_{\text{INP-bio}}$ were excluded from the linear fitting and are marked by solid yellow dots. (d–f) The concentration-weighted trajectory (CWT) analysis for the distribution of $N_{\text{INP-bio}}$ at (d) -10.5°C , (e) -13°C and (f) -16°C .**